Electrolytic Capacitor Current Pulse Networks for Quasi-Steady MPD Arcs

PAUL J. WILBUR*
Colorado State University, Fort Collins, Colo.

A simple model of an equal element *LC* ladder network containing electrolytic capacitors as the energy storage components is presented, and the current waveform predicted by the model for the case of the network discharging through a fixed inductive-resistive load is shown to agree with an experimentally observed waveform. The effect of the series resistance associated with electrolytic capacitors on the efficiency of energy transfer from the network to the load is determined. Using these results, the mass of a power source-pulse network system containing electrolytic capacitors is compared to that of a system which contains nonelectrolytic units and transfers the same power to a quasi-steady MPD arc load. Results of this comparison based on a state-of-the-art component specific masses indicate electrolytic systems are less massive than conventional systems, particularly at low power, long pulse duration conditions.

Nomenclature

A = capacitor surface area (m^2)
C = pulse network intrastation capacitance (farad)
E = energy (joule)
I = current (amp)
K = proportionality constant
L = pulse network intrastation inductance (h)
m = mass (kg)
n = number of elements in pulse network
P_j = power to thruster (w)
Q = charge (coul)
R = resistance (Ω)
t = time (sec)
V = voltage (v)
Z = pulse network impedance (Ω)
α_1 = specific mass of electrolytic capacitors (kg/coul)
α_2 = resistance-capacitance proportionality constant (Ω farad)
α_3 = specific mass of conventional capacitors (kg/joule)
α_4 = specific mass of power source (kg/w)
α_5 = specific mass of radiators (kg/w)
η = efficiency
τ = characteristic pulse duration (sec)

Subscripts

c = conventional system
e = electrolytic system
L = load
o = initial condition
p = in parallel with capacitor
s = in series with capacitor

Introduction

CURRENT interest in the quasi-steady MPD arc thruster has prompted a concomitant search for a power conversion scheme that will permit transformation of the steady energy flow from the primary power source into current pulses of the proper duration and magnitude for operation of the arc. The compatibility of pulse networks composed of the high capacitance, low voltage electrolytic capacitors with the low voltage, long pulse duration, low impedance requirements of the quasi-steady MPD arc has been suggested.[1] Although the electrolytic units have a smaller mass per unit energy stored and their high capacitance, low voltage characteristics are congruent with thruster constraints, they have other characteristics which make them look inexpedient in this application and should be considered in their evaluation. Among these are a high series resistance which results in joule heating losses during discharge operations and a leakage current which could result in significant losses during charging operations. Under the constraint of a fixed thruster output, these losses in the electrolytic network are reflected as an increase in the masses of the primary power source and radiators required to reject heat dissipated in the capacitors over the mass of a system using conventional capacitor elements. These additional masses lessen the mass saving achieved through the use of the electrolytic elements.

Electrolytic capacitors[2] consist of a metallic anode (frequently aluminum or tantalum foil) on which an oxide of the base metal, which is connected electrically to a cathode through a conducting electrolyte, has been deposited. The essential differences between electrolytic and conventional, nonelectrolytic units are:

1) The thickness of the dielectric film in the electrolytic capacitor, formed electrochemically on the surface of the anode, can be controlled to very small values (less than 10^{-6} in.). Since capacitance varies inversely with the thickness of the dielectric this very thin layer results in an extremely large capacitance per unit surface area. The maximum obtainable capacitance in the nonelectrolyte unit is, on the other hand, determined by the thinnest dielectric that can be manufactured with a uniform integrity and still remain intact during construction (generally of order 10^{-4} in.).

2) A relatively large resistance to current flow is observed in electrolytic units while conventional capacitors exhibit a negligible resistance. This series resistance appears to be associated primarily with current flow through the oxide film and the interface between this film and the electrolyte in the electrolytic units.

3) In the neighborhood of its rated voltage the electrolytic capacitor exhibits a marked increase in leakage current associated with the onset of dielectric failure, while this current is negligible in the conventional unit until the dielectric breakdown voltage is reached and catastrophic failure occurs.

Theoretical Network Model

The *LC* ladder network, used extensively to provide current pulses for pulsed electromagnetic thrusters, provides con-

Presented as Paper 70-1082 at the AIAA 8th Electric Propulsion Conference, Stanford, Calif., August 31–September 2, 1970; submitted November 11, 1970; revision received March 11, 1971.

* Assistant Professor, Mechanical Engineering Department. Member AIAA.

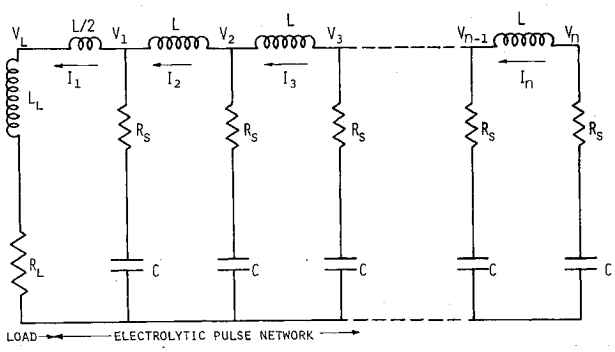

Fig. 1 *LC* ladder network—load schematic.

siderable flexibility in the selection of pulse duration and the pulse network impedance required to effect efficient energy transfer to the thruster. On the basis of this flexibility and the availability of experimental data[1] for comparison with theoretical results, the *LC* ladder network was combined with a fixed inductive-resistance load representing the thruster, to obtain the system illustrated schematically in Fig. 1.

L, C, and R_s represent respectively the intrastation inductance, capacitance, and series resistance for the equal element network. R_L, L_L, and V_L are the load resistance, the inductance associated with the load and its connection to the pulse network (referred to subsequently as the load inductance), and the voltage developed across the load. Similarly the V_i's and I_i's represent voltages across the various capacitor elements in the network and currents passing through the inductors. During initial investigations, circuit elements representing a resistance in parallel (R_p) and a parasitic inductance in series (L_s) with each capacitor in the network were also included in the analysis, but the studies showed no significant effects due to these elements over the range of variation considered ($L_s < 0.05L$, $R_p > 10^3\Omega$). These elements are therefore not included in the schematic and their effect will be neglected in the following discussion.

When Kirchoff's voltage and current relations are applied to the loops and nodes of this network the following equations are obtained:

$$V_L = I_1R_L + L_LdI_1/dt \tag{1}$$

$$V_1 - V_L = (L/2)dI_1/dt \tag{2}$$

$$V_i - V_{i-1} = LdI_i/dt, \qquad i = 2,n \tag{3}$$

$$V_i = Q_i/C - (I_i - I_{i+1})R_s, \qquad i = 1, n-1 \tag{4}$$

$$V_n = (Q_n/C) - I_nR_s \tag{5}$$

$$dQ_i/dt = -I_i + I_{i+1}, \qquad i = 1, n-1 \tag{6}$$

$$dQ_n/dt = -I_n \tag{7}$$

where the Q_i's represent the charges on the capacitors.

Simultaneous solution of these equations has been accomplished using a Runga-Kutta procedure on the digital computer. A typical current waveform obtained by this procedure is presented in Fig. 2 along with experimental results obtained with an electrolytic network and MPD arc as reported in Ref. 1. The pulse line parameters used to obtain the theoretical result of Fig. 2 were the same as those reported for the 20 element experimental network, namely, 1000 μfd capacitors with inductances of $5 \times 10^{-7}h$, discharged from 450 v through a 0.005Ω load resistance. The load inductance was assumed to be $1 \times 10^{-7}h$, and the series resistance used in the analysis was estimated to be 0.27Ω based on manufacturer specifications contained in Ref. 3.

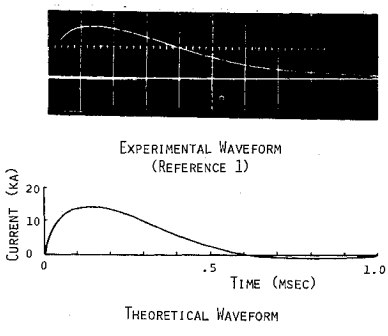

Fig. 2 Current waveform comparison.

The theoretical and experimental waveforms of Fig. 2 show both qualitative and quantitative agreement to within the accuracy permitted by the input parameters except toward the end of the pulse where the experimental waveform shows no current reversal while the theoretical waveform does include a slight negative current. This difference is assumed to be due to the nature of the MPD arc discharge which does not behave as a fixed resistive-inductive load at the beginning and end of the current pulse. This hypothesis is supported by a test performed by the author using polar electrolytic capacitors, similar to those used in the work of Ref. 1, in an *LC* ladder network discharging through a low resistance load in which the current reversal was observed. Based on the agreement between the theoretical and experimental current waveforms, the mathematical representation of the electrolytic pulse network was assumed to be valid, and the effect of the magnitude of the series resistance was examined.

Network Design Considerations

The *LC* ladder network parameters which must be adjusted to assure optimum performance of an "n" element nondissipative network ($R_s = 0$) are the characteristic pulse line impedance ($Z = (L/C)^{1/2}$) and the characteristic pulse time [$\tau = 2n(LC)^{1/2}$]. The optimum performance condition is realized when the characteristic impedance is equal to the load resistance, in which case essentially all of the energy stored initially in the network is transferred to the load within the pulse time (τ). The current waveform obtained under these conditions displays a rapid rise to a constant value ($I_1 = V_o/2Z$, where V_o is the initial network voltage) followed by a sudden drop to the zero current condition as the characteristic pulse time expires. The addition of resistance in series with the capacitors with a magnitude equal to that of the characteristic impedance results in a deformation of the current waveform from the standard rectangular shape to that shown in Fig. 3. The current and time axes in Fig. 3 have been nondimensionalized using the short-circuit current for the nondissipative line (V_o/Z) and the characteristic pulse time respectively. Although the early part of the waveform has the same magnitude and shape as that for the nondissipative network, the series resistance manifests itself in the gradual decay of current at the end of the pulse. This tail becomes more pronounced as either the series resistance is increased or the number of elements in the pulse network is reduced. Similar current waveforms are obtained for other network configurations providing the two ratios (R_L/Z) and (R_s/nZ) are the same.

One would expect the series resistances to dissipate some of the initial pulse line energy, so the maximum obtainable efficiency should be less than that observed with the nondissipative network. This behavior is indeed observed as illustrated in Fig. 4 where the fraction of the initial pulse line energy

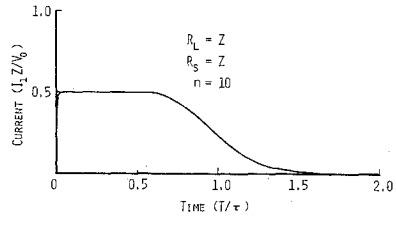

Fig. 3 Current waveform, *LC* ladder network with series resistance.

transferred to a load resistance in a time equal to the characteristic pulse time (τ) is plotted against the relative impedance match ratio. The results are presented parametrically in terms of the similarity parameter associated with the dissipative network, the effective network resistance (R_s/nZ).

For the case where the series resistance is zero, the ideal behavior is observed; peak efficiency occurs when the load resistance is matched to the characteristic pulse network impedance. As the effective network resistance is increased, the maximum energy that can be transferred within the allotted time is reduced as expected, but in addition the relative impedance match condition at which the optimum occurs shifts to higher values of the relative load resistance. Since the load resistance associated with the MPD arc has a fixed value in the range 0.005Ω to 0.010Ω this means the characteristic line impedance must be reduced as effective network resistance increases if peak efficiency is to be realized. The results presented in Fig. 4 were obtained using pulse networks composed of 5, 10, and 20 stations and the results are presumed to apply to any LC ladder network composed of at least 5 equal element stations.

The locus of the maxima of the efficiencies, shown as a dotted line in Fig. 4, is a curve of interest to one designing a pulse network, but it is not a convenient form because the variables have been nondimensionalized using the characteristic impedance, when it is the effective load resistance (thruster impedance) that is generally fixed. In Figs. 5 and 6 the pulse line impedance required to achieve peak efficiency and the efficiency have been plotted against the network resistance, and both the effective resistance and nondissipative impedance for the network have been nondimensionalized using the load resistance. The parameter in these curves is the time at which the efficiency is evaluated, expressed in terms of characteristic pulse time. As expected the efficiency can be increased by allowing a longer period of time for the network to discharge. This increase is most significant when the series resistance is large and the resulting tail of the current waveform is long.

The reduction in characteristic line impedance required to achieve peak efficiency as effective network resistance is increased is quite significant as shown in Fig. 5. A series resistance of about 0.025Ω in the elements of a 10 element network driving a 0.005Ω load would for example require a pulse network with an impedance in the range of 0.002Ω and less than 50% of the initial energy would be deposited in the load.

The results presented in Figs. 4–6 were obtained assuming a negligible load inductance so the rise time of the current in these cases is determined by the line inductance associated with the first station in the network (see Fig. 1). The effect of load inductance is to increase the time required for energy transfer. The extent of this increase is determined by the magnitudes of the load inductance, the effective network resistance and the relative impedance match.

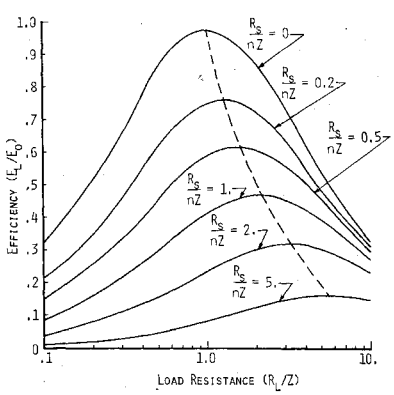

Fig. 4 Effect of relative impedance match and series resistance on efficiency ($t = \tau$).

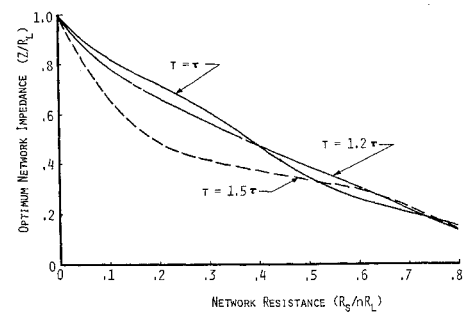

Fig. 5 Effect of network resistance on line impedance for maximum efficiency.

Scaling Electrolytic Capacitor Variables

Since foil and spacer thicknesses in electrolytic capacitors are generally fixed by physical strength and heat conduction considerations associated with their construction and operation, the mass of each capacitor (m_e') may be assumed to scale directly with its surface area (A)

$$m_e' = K_1 A \tag{8}$$

The capacity (C_e/A) of these units is related to the anode formation voltage[2,4] (V_f) applied during manufacture by the equation,

$$C_e/A = K_2/V_f \tag{9}$$

The operating voltage (V_o) is also related to the anode formation voltage by the equation,

$$V_o = K_3(1 - e^{-K_4 V_f}) \tag{10}$$

Combining Eqs. (8, 9, and 10) the capacitor mass can be related to the capacitance and breakdown voltage by the equation:

$$m_e' = (-K_1/K_2K_4)C_e \ln[1 - (V_o/K_3)] \tag{11}$$

Assuming K_3 is sufficiently greater than V_o so that higher order terms may be neglected, one obtains:

$$m_e' \approx \alpha_1 C_e V_0 \tag{12}$$

This result agrees with information contained in Ref. 2 which states that electrolytic capacitor volume scales directly with its charge carrying capability. Measurements made on available electrolytic units suggest α_1 might have a value as low as 1.3 kg/coul.

It appears that the bulk of the series resistance associated with electrolytic capacitors is found in the dielectric film, with additional less significant contributions arising from characteristics of the film interfaces and the electrolyte.[2,5] This suggests that the resistance of electrolytic capacitors scales directly with the film thickness and inversely with the film surface area, and since the capacitance scales directly with the area and inversely with film thickness, the capacitance and

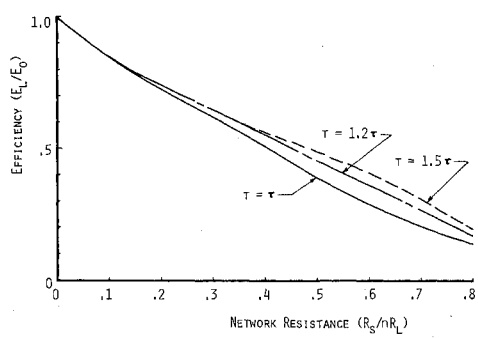

Fig. 6 Variation of maximum efficiency with network resistance.

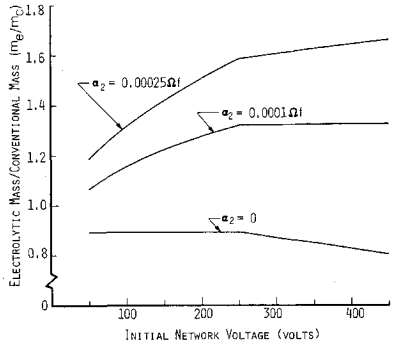

Fig. 7 Mass comparison of electrolytic and conventional pulse network—primary power source systems, P_j = 10 kw, "τI_1" = 5 coul.

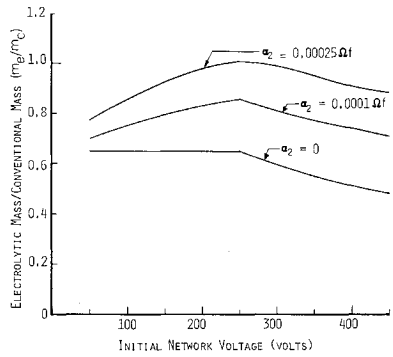

Fig. 9 Mass comparison of electrolytic and conventional pulse network—primary power source systems, P_j = 10 kw, "τI_1" = 25 coul.

series resistance of electrolytic capacitors should satisfy the relation:

$$R_s = \alpha_2/C_e \tag{13}$$

Comparison of series resistances predicted by this equation with those included in manufacturer specifications[3] show a close correspondence when μ_2 lies in the range around 0.00025Ω farad.

Mass Comparisons

In order to provide a valid comparison between the mass of an MPD thruster system using electrolytic capacitors and one which employs conventional (nonelectrolytic) units it is necessary to consider the masses of the capacitors, powerplants, and radiators required to dissipate heat generated in the capacitors under the constraint of a fixed power output to the thruster (P_j). Initial investigations showed that losses associated with the leakage current observed during electrolytic capacitor charging operations resulted in an inconsequential energy loss.

The mass of primary power source and conventional pulse network (m_c) operating a thruster at an average power level, P_j, may be assumed to scale according to the relation:

$$m_c = \alpha_3(n_c C_c V_0^2/2) + \alpha_4 P_j \tag{14}$$

Lossless energy transformation through the conventional pulse network has been assumed through Eq. (14) in that thruster input is equated to primary power source output. Scaling the mass of a conventional pulse network composed of n_c units of capacitance C_c at a discharge voltage of V_o in proportion to the energy stored in the capacitors is generally accepted at high voltages, but its validity at low voltages requires some justification. Dielectric breakdown studies made using crystals[6] suggest breakdown strength increases as dielectric thickness is reduced. This behavior would correspond to a reduction in α_3 with decreases in dielectric thickness, and, hence, rated voltage. Although this behavior may also be observed in polymer film dielectrics, it appears that the breakdown strength is independent of thickness[7] and that the scaling suggested in Eq. (14) will therefore remain valid at low voltages. At these low voltages, however, the minimum thickness of the dielectric that can be made and handled during construction becomes the limiting factor. Mylar has been formed into sheets as thin as 0.000025 in. for capacitor construction applications.[8] Combining this with the fact that two layers of film are generally used to prevent breakdown due to slight variations in film properties and the fact that the dielectric strength of Mylar is 5×10^6 v/in., a minimum breakdown voltage of 250 v is predicted. The mass of a capacitor operating below this voltage would therefore still be determined by the 250 v rating.

For the lossless pulse line at the peak efficiency condition the discharge current is given by:

$$I_1 = V_o/2Z = n_c C_c V_o/\tau \tag{15}$$

Combining this with Eq. (14) yields

$$m_c = (\alpha_3 \tau I_1 V_o/2) + \alpha_4 P_j \tag{16}$$

In order to assure quasi-steady arc operation, "τI_1" $\geq$ 5 amp sec is required.[1] Since the product "τI_1" appears in the numerator of Eq. (16), it is apparent that the minimum system mass will be realized when this product assumes its minimum value.

The mass (m_e) of the primary power source and electrolytic pulse network again operating a thruster at an average power level, P_j, when the efficiency of energy transfer from the pulse network is η_e, is given by:

$$m_e = \alpha_1 n_e C_e V_o + (\alpha_4 P_j/\eta_e) + \alpha_5 P_j[(1/\eta_e) - 1] \tag{17}$$

The first term of this equation represents the mass of the electrolytic network composed of n_e elements and follows the

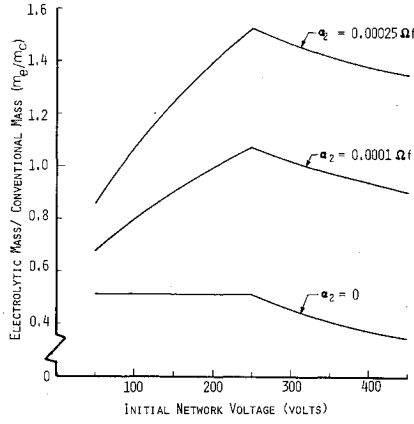

Fig. 8 Mass comparison of electrolytic and conventional pulse network—primary power source systems, P_j = 1 kw, "τI_1" = 5 coul.

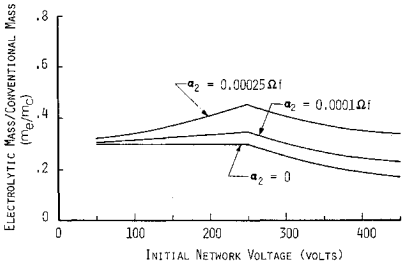

Fig. 10 Mass comparison of electrolytic and conventional pulse network—primary power source systems, P_j = 1 kw, "τI_1" = 25 coul.

scaling expression [Eq. (12)] developed previously. The second term represents the mass of the primary power source required to operate the thruster at an average power P_j, and the third term the mass of radiators required to reject heat deposited in the electrolytic capacitors. When one assumes values for the pulse line voltage (V_o), thruster power (P_j) and the coefficients (α_1, α_2, α_4, and α_5), Eqs. (17) and (13) together with Fig. 6 yield a capacitance (C_e) which corresponds to a minimum system mass. The number of pulse line elements (n_e) may be assigned any reasonable value because it appears in both Eq. (17) and as an argument in Fig. 6 and simultaneous solution reveals the resultant minimum system mass is independent of the number of pulse network elements.

The following values of proportionality constants and thruster characteristics have been selected as typical of a state-of-the-art MPD thruster and capacitors operated from a solar-electric power source: $\alpha_1 = 1.3$ kg/coul; $\alpha_3 = 0.05$ kg/joule; $\alpha_4 = 0.02$ kg/w; $\alpha_5 = 0.005$ kg/w; $R_L = 0.005\Omega$.

Application of these in Eqs. (13, 16, and 17) and Fig. 6 enables one to determine the ratio of masses for conventional and electrolytic systems as a function of pulse line voltage (V_o), thruster power (P_j), pulse line charge (τI_1) and electrolytic capacitor resistance-capacitance proportionality constant (α_2). Results of these calculations are presented in Fig. 7 for the case where thruster power is 10 kw and the pulse line charge assumes the minimum allowable value of 5 coul. In the upper curve the constant of proportionality between series resistance and capacitance of the electrolytic units is in the range suggested by manufacturer specifications[3] ($\alpha_2 = 0.00025\Omega$ farads at 120 cps). Experimental data obtained recently from electrolytic capacitors intended for assembly into a pulse line configuration suggest however that the series resistance associated with these units evaluated under discharge conditions is considerably less than the value cited in manufacturer specifications.[9] This agrees with the information of Ref. (5) which notes that the dominant part of this resistance is associated with the dielectric film and that its magnitude varies inversely with frequency. Since the extent of this reduction is not known, additional curves shown in Fig. 7 correspond to $\alpha_2 = 0.0001\,\Omega$ farad and the limiting case of nondissipative electrolytic capacitors ($\alpha_2 = 0$).

As shown in Fig. 7, for this particular set of conditions, the electrolytic system is more massive unless the series resistance can be reduced an order of magnitude below the 120 cps manufacturer specifications.

Two additional points should be made regarding Fig. 7. They are: 1) The break in the curves at 250 v occurs because the mass of the conventional units is constrained until this minimum breakdown voltage condition, described earlier, is exceeded. 2) The charge stored in the electrolytic network is in excess of the 5 coul limit because over-all electrolytic system mass tends to minimize at high capacitance (and charge) values where series resistance and hence primary power source mass are lower.

Figure 8 presents the same comparison as that given in Fig. 7 but the average thruster power has been reduced to one kilowatt. At this lower power the pulse network masses represent a larger fraction of the total system mass and as illustrated in Fig. 8, this facilitates a reduction in the mass ratio and therefore favors the electrolytic system.

Figures 7 and 8 correspond to what is considered the minimum acceptable pulse line charge required to assure quasi-steady operation of the thruster. When the total charge assumes this minimum value the conventional pulse system assumes a corresponding minimum mass. Since the electrolytic system mass is minimal at somewhat higher charges, this restriction favors the conventional network.

If one assumes some improvement in thruster performance could be achieved by going to larger operating times (increase in charge) a comparison of system masses at higher values of pulse network charge is of interest. Data presented in Figs. 9 and 10 were obtained using a total charge ("τI_1") of 25 coul. These curves demonstrate the same qualitative behavior as that presented in Figs. 7 and 8, and they confirm the proposition that the conventional network is favored by high-power, low total network charge operating conditions.

Conclusion

The effect of the series resistance associated with electrolytic capacitors is to dissipate energy and hence reduce the efficiency of energy transfer from an LC ladder network to a load. These losses can be minimized if the pulse network is designed such that its characteristic impedance is reduced to progressively lower values as series resistance increases.

The mass of an electrolytic pulse network and primary power source required to operate a given MPD thruster is determined to a large extent by the proportionality constant between series resistance and capacitance. Using reasonable values of this constant and state-of-the-art component specific masses leads to the conclusion that electrolytic systems are less massive than conventional ones at thruster power levels less than about 10 kw. Electrolytic systems are favored by operation at high pulse line charge conditions (corresponding to long pulse durations at given current levels) and low power (where pulse line mass is comparable to powerplant mass).

Future trends in this mass comparison will be determined to a large extent by the success of efforts, 1) to reduce the series resistance of electrolytic capacitors, and 2) to build conventional capacitors more closely matched to the low voltage needs of the quasi-steady MPD arc.

References

[1] Ducati, A. C. and Jahn, R. G., "Repetitively-Pulsed Quasi-Steady Vacuum MPD Arc," AIAA Paper 70-167, New York, 1970.

[2] Georgiev, A. M., *The Electrolytic Capacitor*, Murray Hill, New York, 1945, Chaps. 2,5.

[3] *Sprague Engineering Bulletins* 3431B and 3441D, Sprague Electric Company, North Adams, Mass.

[4] Ruben, S., "History and Development of Dry Electrolytic Capacitors," *Electrochemical Technology*, Vol. 3, No. 11–12, Nov.–Dec. 1965, p. 301.

[5] Ho, R. K., "Solid Electrolytic Tantalum Capacitors—Index of Quality," *Insulation*, Vol. 13, No. 3, March 1967, pp. 69–73.

[6] O'Dwyer, J. J., *The Theory of Dielectric Breakdown of Solids*, Oxford University Press, London, 1964, pp. 99–104.

[7] Blok, J. and Legrand, D. G., "Dielectric Breakdown in Polymer Films," *Annual Report: Conference on Electrical Insulation and Dielectric Phenomena*, National Research Council Publication 1484, National Academy of Science, 1967, pp. 18–22.

[8] Kahn, L., "Dielectrics in Capacitors," *Dielectric Materials and Applications*, edited by A. R. von Hippel, The M.I.T. Press, Cambridge, Mass., 1954, pp. 221–225.

[9] Villani, D., "Electrolytic-Capacitor Pulse-Forming Network," *Pulsed Electromagnetic Gas Acceleration*, AMS Rept. 634n, Jan. 1970, Princeton University, Princeton, N. J., pp. 36–40.